PCCP

Accepted Manuscript

ROYAL SOCIETY OF CHEMISTRY

www.rsc.org/pccp

Physical Chemistry Chemical Physics

Dynamic Article Links ►

Cite this: DOI: 10.1039/c0xx00000x

www.rsc.org/xxxxxx

Communication

Simultaneous glucose sensing and bio-hydrogen evolution from direct photoelectrocatalytic glucose oxidation on robust Cu_2O-TiO_2 electrodes

Anitha Devadoss,[a] P. Sudhagar,[a*] C. Ravidhas,[c] Ryota Hishinuma,[a,b] Chiaki Terashima,[a,c*] Kazuya Nakata,[a,b,c] Takeshi Kondo,[a,b,c] Isao Shitanda,[a,b,c] Makoto Yuasa[a,b,c] and Akira Fujishima[a,c]

Received (in XXX, XXX) Xth XXXXXXXXX 20XX, Accepted Xth XXXXXXXXX 20XX

DOI: 10.1039/b000000x

We report, simultaneous photoelectrocatalytic (PEC) glucose sensing and bio-hydrogen generation for the first time from direct PEC oxidation of glucose at multifunctional and robust Cu_2O-TiO_2 photocatalysts. Striking improvement of 30% in overall H_2 gas evolution (~122 µmol.hr^{-1}cm^{-2}) by photoholes assisted glucose oxidation opens new platform in solar-driven PEC bio-hydrogen generation.

Light driven photosensitized water oxidation phenomenon[1] is the key tool for accessing the photoholes at the valence band of semiconductor to advanced oxidation of chemical components in liquid or gas phase.[2-4] In this context, direct photoelectrocatalytic (PEC) oxidation of glucose using semiconductor is an interesting approach to reforming the biomass into hydrogen fuel through artificial photosynthesis process.[5-9] Previous reports on Pt decorated TiO_2 in the form of powder[10] as well as electrode[11] demonstrated the ability of 'photoholes' towards glucose oxidation for generating useful fuel such as hydrogen and oxygen. Although, metal (Pt) particles facilitate the charge separation at TiO_2/electrolyte interface, (a) the light blocking effect by Pt, (b) undesirable CO_2 generation through photo-Kolbe reaction that leads to poor selectivity in H_2 generation and (c) inadequate photoholes conduction at TiO_2 limits the practical implementation. Conversely, p-type semiconductors are the promising candidates in PEC water splitting process for collecting photoholes efficiently to Pt counter electrode. Nonetheless, developing a robust p-type semiconductor photoelectrode is currently a key challenge in the field of PEC biosensors and bio-fuel generation. In this context, cuprous oxide (Cu_2O), a p-type metal oxide with a band gap of ~2-2.6 eV is currently extensively studied in photocatalyst, solar cells, photosensor applications.[12,13,14, 15] Despite their good photoactivity, high binding energy, affordability and abundance occurrence, its photocorrosive tendency due to high native Cu vacancies[16, 17] remains a significant drawback. Thus, it is significant to improve the Cu_2O stability for efficient biomolecular oxidation. Recently, it has been reported that Cu_2O photocathode stability can be improved by post-coating thin layers of metal oxide (TiO_2),[18, 19] or carbon materials,[13] which may improve the PEC performance. On this note, electron conducting and transparent coatings of TiO_2 is an appropriate choice owing to the negligible obstruction of light reaching the photoactive Cu_2O layer.[20] In addition, the presence of TiO_2 layer on Cu_2O could also facilitate the charge separation and electron transfer at electrode/electrolyte interfaces. Therefore, synergistic combination between single-oxide properties, such as low band-gap p-type Cu_2O and high reactivity of n-type TiO_2 could be the most appealing alternative for improving the PEC efficiency.[21]

Glucose plays a vital role of a biomarker in the clinical therapy of diabetes.[22] The recent substantial development of sensing technologies suggest the use of enzymes or noble metal catalysts for the successful oxidation of biomolecules;[23,24] however, the stability and price remain intrinsic restrictions.[25] Moreover, glucose is a well-recognised biofuel source which is low-cost, renewable and available as waste products of biomass processing industries (sugar, pulp and paper), which makes it an attractive sustainable source of bio-hydrogen.[26] Despite the great progress achieved in hydrogen production from biomass over the past decades, there still remain significant challenges to design efficient, enzymeless and cost-effective means of producing hydrogen at exceptionally mild conditions.

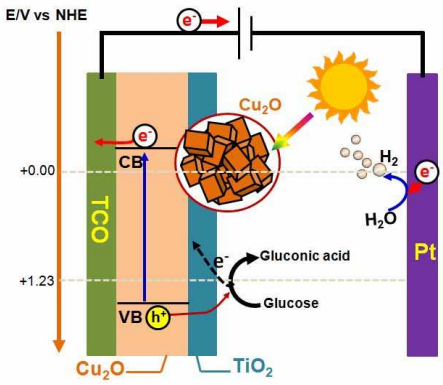

Scheme 1. Illustration of direct photoelectrochemical glucose oxidation at Cu_2O/TiO_2 electrode. The electrons collected from both glucose electrooxidation and photocatalytic oxidation to the counter electrode by applied potential 0.7 V vs (Ag/AgCl).

Herein, we demonstrate for the first time, the simultaneous photoelectrochemical glucose biosensing and bio-hydrogen generation from direct PEC oxidation of glucose at highly stable

and sensitive Cu_2O-TiO_2 photoelectrodes. The PEC process of simultaneous glucose oxidation at Cu_2O-TiO_2 photoelectrodes and bio-hydrogen generation at Pt counter is proposed in **Scheme 1.** Under dark condition, the Cu_2O primarily acts as electrocatalyst towards glucose oxidation at applied potential (0.7 V vs Ag/AgCl). This potential is substantially enough to achieve flat band at Cu_2O/TiO_2/electrolyte interfaces, and thus capable of collecting the oxidative electrons (dotted arrow in Scheme 1) to the collector terminal through Cu_2O and TiO_2 layers. Upon light illumination with similar applied potential, Cu_2O acts as photoelectrocatalyst, which generates photoelectrons at conduction band (CB) and photoholes at valence band (VB). The photoholes from VB lying just positive of the oxygen evolution potential (+1.23 eV NHE) substantially drives the glucose oxidation. This photocatalytic glucose oxidation beneficially promotes the oxidative electrons (dotted arrow in Fig.1a). Concurrently, fraction of photoelectrons will be injected in to the collector terminal, thus raise the overall bio-hydrogen evolution (bio-fuel) at Pt counter electrode.

The Cu_2O-TiO_2 photoelectrodes used in this study were prepared by forming CuO layer on transparent conducting oxide (TCO) substrate using spray pyrolysis process followed by sputter coating a thin layer of TiO_2 (**See supporting information S1**). The crystalline structure of as-prepared CuO films was studied using x-ray diffraction technique (Fig.1a). Two predominant peaks exhibited in Fig. 1a, at 35.3º and 38.4º, confirm the (002) and (111) crystallite phases, respectively corresponding to the tenorite structure CuO (JCPDS 45-0937).[27, 28]

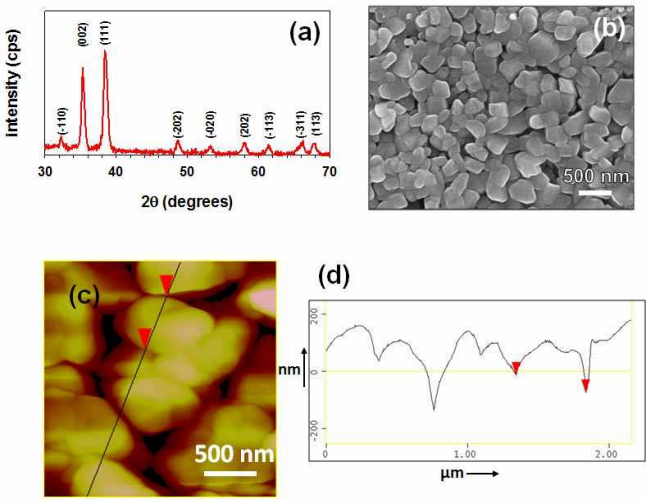

Fig.1. (a) X ray diffraction spectrum, (b) SEM image and (c) AFM image of spray coated CuO film; (d) AFM section analysis on CuO crystals across the line indicated in Fig.1(c).

The surface morphology of CuO films shows quasi crystallite shape (Fig.1b). Further, this quasi crystallite texture was confirmed by atomic force microscope (AFM) (Fig. 1c). From AFM section analysis, it is found that CuO crystals have distinct dimension of ~492 nm in diameter and ~ 395 nm in height. The chemical environment of CuO films before and after TiO_2 coating was studied by x-ray photoelectron spectrometer (XPS) and the corresponding results were presented in Fig. 2 (a) and (b). In pristine CuO films, predominant $Cu2p_{3/2}$ (933.2 eV) and $Cu2p_{1/2}$ (953.2 eV) peaks along with two strong satellite (SS) peaks were observed. These Cu2p strong satellite peaks at 949.1 eV and 961.9 eV correspond to the $Cu2p_{3/2}$ and $Cu2p_{1/2}$, respectively.[29]

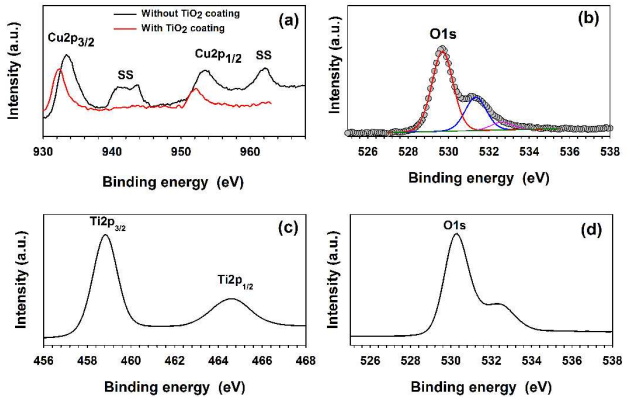

Fig.2. XPS results of CuO films (a) Cu2p [with and without TiO_2 post-deposition]; (b) O1s core spectra without TiO_2 coating; (d) Ti 2p core spectra and (e) O1s core spectra of CuO films with TiO_2 coating.

Furthermore, the atomic ratio of Cu and O was estimated from XPS spectra and found to be 0.3 and 0.7 Wt %, respectively. The shoulder peaks of $Cu2p_{3/2}$ and $Cu2p_{1/2}$ were shifted to lower binding energy implying that the CuO surface gets modified by TiO_2 post-deposition. Moreover, the SS peaks of CuO were disappeared upon TiO_2 post-deposition. This tendency indicates the Cu_2O phase formation (Cu^{2+} to Cu^{+} ions) in between TiO_2 and CuO.[30, 31] It is reported that the CuO phase transformation might occur either from chemical state interactions at two different oxide phase interface[32] or applying oxidation treatment on CuO surface[31]. The plausible reason for Cu_2O phase formation might originate from the oxygen species during TiO_2 sputtering process could interact with CuO surface and thus form thin layer of Cu_2O in between CuO and TiO_2 (this thin Cu_2O layer was not observed from XRD spectra). Under this circumstance, the half-filled d^9 configuration in the ground state of CuO might get filled by oxygen species during sputter deposition. Therefore the screening of charge transfer into the d-states result disappearance of SS peaks at CuO-TiO_2 electrode, which is in agreement with previous report.[33] The O1s peak of CuO film (Fig.2d) was de-convolute into two peaks at 529.8 eV and 531.2 eV, which represents the Cu=O and intrinsic oxygen defects in the crystal lattice, respectively.[34] The presence of TiO_2 on CuO layer was confirmed by the presence of Ti 2p and O1s peak from TiO_2 coated CuO sample (Fig. 2c and 2d). Consequently, the TiO_2 post-deposition switched the hydrophobic nature of CuO films (contact angle ~ 132.8º) ino hydrophilic (contact angle ~ 76.7º) surface (**See Supporting information Fig. S2**). From the above discussion, it concludes that the Cu_2O layer may form in between the CuO and TiO_2. Hereafter, TiO_2 coated CuO electrodes will be coined as Cu_2O-TiO_2.

The electrochemical (EC) and photoelectrochemical (PEC) response of CuO and Cu_2O-TiO_2 photoelectrodes in the presence and absence of glucose were examined using cyclic voltammetry as shown in Fig. 3(a) and (b), respectively. The aqueous solution of 0.1 M NaOH was used as electrolyte and the experiments were conducted at 50 mV/s scan rate. In the absence of glucose, the

CuO electrode showed dark current density ~1.6 mAcm^{-2} at negative applied potential of -0.55 V vs (Ag/AgCl). Upon light illumination, the photocurrent density value was enhanced to ~3.7 mAcm^{-2}. This explains the complete photoelectrocatalytic water splitting on CuO surface (using photoelectrons at CB) and water oxidation at Pt surface through collecting the photoholes from VB of CuO. This ensures the photoelectron and photohole generation at CuO under illumination with negative potential.[35] On the other hand, the current density showed ~1.6 mAcm^{-2} at positive applied potential 0.7 V vs (Ag/AgCl) is related to hydrogen generation on Pt surface as is explained in Scheme 1. Strikingly, the current density was enhanced to ~7.9 mAcm^{-2} (dark condition) in presence of 5 mM glucose in electrolyte. This infers that the electrooxidation of glucose takes place at CuO surface at 0.7 V vs (Ag/AgCl), where glucose is converted into gluconic acid.[36] This process exhibits one electron to the external circuit (dotted arrow in Scheme 1) and thus raises the current nearly fivefold compared to electrolyte without glucose. Nonetheless, no change in current density was observed under light illumination. This may be due to the poor charge separation (electron and hole) after photocarrier generation due to photocorrosion issue on CuO surface, since the redox potentials for the reduction and oxidation of copper oxide lie within the bandgap.[18]

$$CuO+H_2O+\ 2e^- \leftrightarrow 2Cu +2OH^-\ (E^o = +0.47\ V) \qquad (1)$$

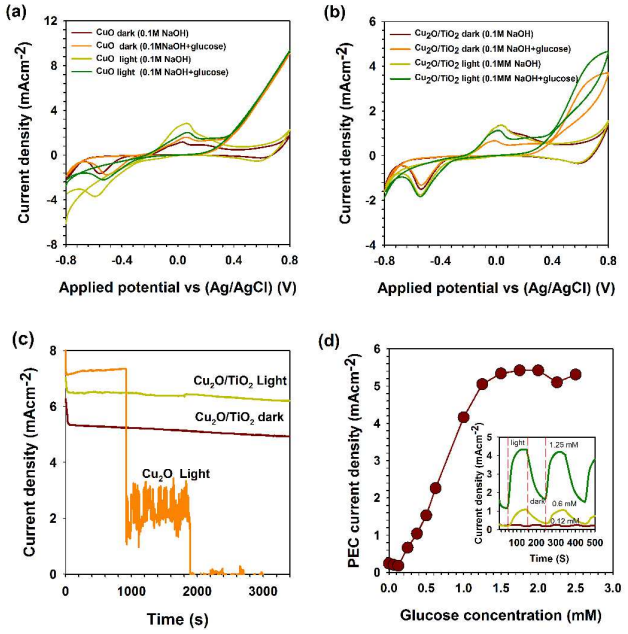

Fig.3. CV results of (a) CuO and (b) Cu_2O-TiO_2 electrodes measured under dark and light illumination condition; (c) chronoamperometric results of glucose oxidation process using pristine Cu_2O and Cu_2O/TiO_2 electrodes; (d) photoelectrocatalytic current response of Cu_2O-TiO_2 electrodes at 0.1 M NaOH aqueous electrolyte with different concentration of glucose (scan rate: 50 mV/s), inset: the photocurrent response of glucose measured at 0.7 V applied potential.

Therefore, photoholes at VB of CuO is inefficient to drive the photocatalytic oxidation of glucose due to detrimental corrosive effect (equation 1). Unlike pristine CuO, the Cu_2O-TiO_2 photoelectrode exhibited significant (Fig.3b) current density difference between the dark (~3.6 mAcm^{-2}) and light illumination (~4.6 mAcm^{-2}) conditions in 5 mM glucose, which clearly demonstrates that TiO_2 deposition on CuO triggers the photocatalytic oxidation of glucose (dotted arrow indicated in Scheme 1). Here, TiO_2 acts as passivation layer and prevents the corrosion. Another plausible reason for enhancing the current density could be the resultant band gap energy tailoring from ~2.2 eV to ~1.82 eV, (**See supporting information S3**) which could maximize the visible light harvesting photons for photocatalytic glucose oxidation process through converting their crystalline phase to Cu_2O as is explained from XPS results (Fig.1c).

In order to realize the stability of electrodes, we have performed the electrocatalytic experiments using CuO and Cu_2O-TiO_2 electrodes in both dark and light illumination conditions (Fig.3c). The Cu_2O-TiO_2 electrode showed excellent stability and reliable performance in both dark and light conditions. Initially, the CuO electrode showed high current density than that of Cu_2O-TiO_2, but later it was found to be degrading rapidly and almost no current was generated after 2000 sec. This clearly evidence that the TiO_2 post-deposition acts as passivation layer to CuO and thus prevents the corrosion and thus affords prolonged operation in both dark and light illumination environment. The stable performance and photocurrent enhancement observed at Cu_2O-TiO_2 electrodes in presence of glucose further encouraged us to testify the PEC sensing ability at different glucose concentrations. Fig.3d shows the dependence of photocurrent with that of the glucose concentration. The inset shows the typical time-based photocurrent response of direct PEC glucose biosensor at lower and higher glucose concentration. The calibration curve shows a linear increase in photocurrent between 375 µM to 1.5 mM glucose and reaches the saturation at about 2.5 mM glucose. This wide linear range with 250 µM detection limit attests the direct PEC glucose sensing ability of Cu_2O-TiO_2 photoelectrodes. The interference analysis shows negligible impact in presence of ascorbic acid and dopamine and thus demonstrates the selective photoelectrocatalytic oxidation of glucose at robust Cu_2O-TiO_2 photoelectrodes (**See Supporting information Fig. S4**). The photocurrent conversion efficiency (PCE) of the Cu_2O-TiO_2 photoelectrode was estimated from Fig.3(b) using the following relation;[37]

$$PCE = [(1.23\text{-}V_{bias})I / (PA)]\times 100 \qquad (2)$$

The V_{bias} is the applied potential between counter electrode and photoanode and calculated using the relation $E_{RHE}= E_{Ag/Agcl}+0.197+pH(0.059)$. The pH of the 0.1M NaOH electrolyte is 11. I is the current density achieved from PEC process. P is the power of the light source (100 mWcm^{-2}). A is the area of the electrode (1 cm^2). The estimated PCE is presented in Fig.4. The maximum PCE of water oxidation performance in Cu_2O-TiO_2 was achieved ~0.8% at ~0.85 V RHE (in the absence of glucose). At high applied potential ~1.23 V RHE, the PCE value is found to reduce ~0.05% due to most of the water molecules were oxidized at lower potential ~0.85V though Cu_2O-TiO_2 can have wide window potential. In the case of glucose included electrolyte, at similar potential ~1.23 V RHE, the PCE of ~0.35% was achieved compared to glucose-free electrolyte. This implies that Cu_2O-TiO_2 electrode have feasibility of direct glucose

oxidation at ~1.23 V RHE and promotes the overall hydrogen generation at Pt CE through supplying additional electrons in to the circuit.

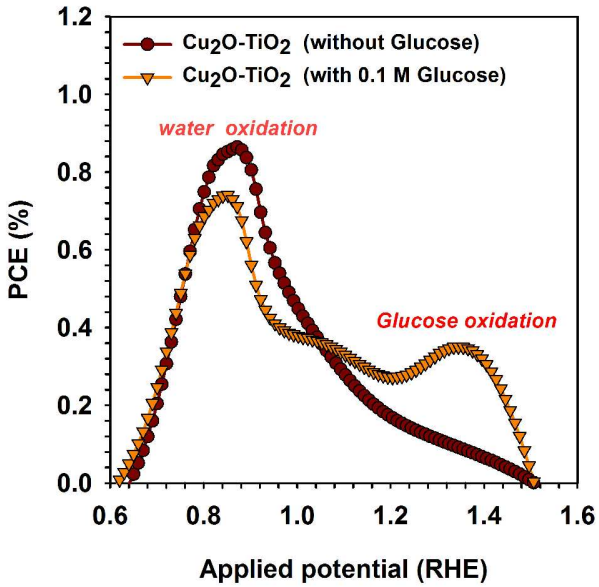

Fig. 4. Photocurrent conversion efficiency of CuO-TiO_2 photoelectrode as a function of applied potential.

The feasible PEC current generation from glucose based electrolyte (Fig. 3c and d) endorse the possible fuel generation. As is explained in Fig.1a, the electrons collected from both electrooxidation of glucose and photoelectrocatalytic oxidation of glucose can be traversed to Pt electrode and thus utilized for bio-hydrogen generation. This phenomenon was testified in three electrode photoelectrochemical system. The output gas evolved for a period of one hour from both EC and PEC glucose oxidation on Cu_2O-TiO_2 electrodes were collected and analyzed by gas chromatography (GC) (Fig. 4a). The GC spectra show well-defined peak of H_2 and peak intensity was enhanced upon light illumination. Our results endorse that the H_2 fuel generation from electrocatalytic glucose oxidation was further promoted with photocatalytic glucose oxidation. The other two peaks in Fig.4a correspond to atmospheric O_2 and N_2 during the sample collection. Further, the quantity of H_2 fuel evolved from Cu_2O-TiO_2 photoelectrodes under different experimental conditions were estimated from GC spectra and are presented in Fig.4b. The Cu_2O-TiO_2 electrodes exhibit small quantity of H_2 (~16 $\mu mol.hr^{-1}cm^{-2}$) gas from direct water splitting phenomena (without glucose). In presence of 2.5 mM glucose in the electrolyte, ~96 $\mu mol.hr^{-1}cm^{-2}$ of H_2 fuel was generated at Pt in dark which could be attributed to the direct electrochemical glucose oxidation. Interestingly, the PEC oxidation of glucose generated the maximum quantity of H_2 gas, ~122 $\mu mol.hr^{-1}cm^{-2}$. This clearly demonstrates that the photoholes generated at valence band of Cu_2O additionally drives glucose oxidation, which beneficially traverses more electrons to the external circuit (Scheme 1), and thus promotes the overall H_2 fuel generation by ~30%. The contribution of photocatalysis phenomena on glucose oxidation using Cu_2O/TiO_2 electrode is in agreement with recent demonstration of suspended photocatalytic glucose reformation using different crystal facet of Cu_2O.[15] The similar hydrogen generation performance from glucose biofuel cells has been summarized by lu et al.[38] The yield of hydrogen product can be doubled from PEC glucose oxidation process while using tandem photoelectrodes. Esposito et al demonstrate the tandem electrode based glucose biofuel cell using WO_3 and CdTe photoanode with tungsten carbide (WC) photocathode.[39] By utilizing co-catalyst ($Ni(OH)_2$) materials on anode surface (TiO_2, Fe_2O_3) could reduce driving potential is an another attractive strategy for improving the glucose bio-fuel cells.[40, 41]

Despite all of the evidences for substantial amount of bio-hydrogen generation, the Cu_2O-TiO_2 system still demands further excellence in terms of detection range as well their stability in industrial biomass waste. Further research is underway to improve their detection range via enhancing the physical active area or internal surface area of Cu_2O-TiO_2 electrodes. Moreover, analysing the stability of Cu_2O-TiO_2 electrodes using industrial biomass waste as feed stock is futuristic for realizing the artificial photosynthesis in bio-hydrogen generation. When compared to the conventional biomass reformation techniques (steam gasification, fast pyrolysis or supercritical conversion) which demands high temperature, undoubtedly, the direct photoelectrocatalytic glucose oxidation using visible light candidates afford low-cost biomass reformation. The central part of the results on glucose sensing with hydrogen generation can be transformed to designing self-powered sensors using the output hydrogen and atmospheric oxygen in the form of fuel cells.

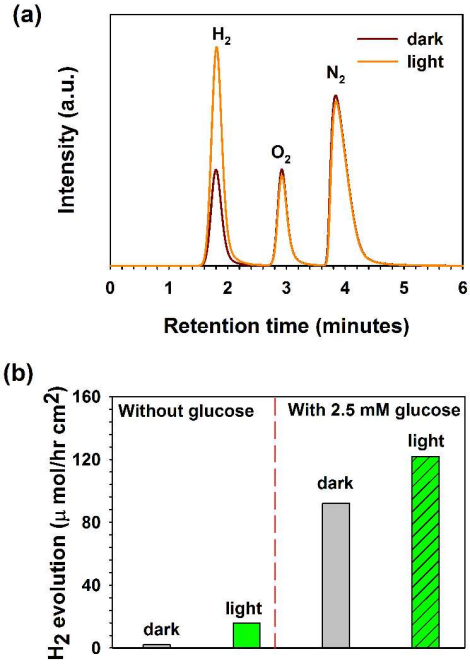

Fig. 5. (c) Typical GC trace of evolved hydrogen gas from the electrochemical glucose oxidation experiments using Cu_2O/TiO_2 electrodes under dark and light illumination conditions (2mM glucose

was included in the electrolyte); (b) measured amount of hydrogen gas from electrochemical and photoelectrochemical measurements using Cu_2O/TiO_2 electrodes in different conditions (1 mM NaOH aqueous solution with 2.5 mM glucose is used as electrolyte; 0.7 V is applied to potential for all experiments).

In conclusion, we have developed multifunctional and highly stable Cu_2O-TiO_2 photoelectrode for direct photoelectrocatalytic oxidation of glucose. This material combination allows for spontaneous direct PEC oxidation of glucose under light illumination, in which photoholes are utilized for enhanced glucose oxidation. The high magnitude photocurrent of about ~4.6 $mAcm^{-2}$ was generated in presence of 5mM glucose. Moreover, simultaneous bio-hydrogen generation from direct PEC oxidation of glucose was demonstrated, which can serve either as an excellent alternative technique in biomass reformation or self-powered biosensors using the output hydrogen and atmospheric oxygen in the form of fuel cells.

Acknowledgements

One of the corresponding authors P.S appreciate the JSPS for provide the post-doctoral fellowship. R.D would like to acknowledge the support of UGC, New Delhi, India (UGC F.No. 42-903/2013 (SR)) for their financial support.

Notes and references

[a] *Photocatalysis International Research Center, Research Institute for Science & Technology, Tokyo University of Science, 2641 Yamazaki, Noda, Chiba 278-8510, Japan,; E-mail: vedichi@gmail.com*
[b] *Faculty of Science and Technology, Tokyo University of Science, 2641 Yamazaki, Noda, Chiba 278-8510, Japan,*
[c] *Department of Physics, Bishop Heber College, Trichy 17, Tamilnadu, India*
[d] *ACT-C/JST; E-mail: terashima@rs.tus.ac.jp*

† Electronic Supplementary Information (ESI) available: [Experimental and characterization details, surface wetablity, optical band gap energy, glucose sensitivity results]. See DOI: 10.1039/b000000x/

1. A. Fujishima and K. Honda, *Nature*, 1972, 238, 37-38.
2. A. Fujishima, T. N. Rao and D. A. Tryk, *Journal of Photochemistry and Photobiology C: Photochemistry Reviews*, 2000, 1, 1-21.
3. M. A. Fox and M. T. Dulay, *Chemical Reviews*, 1993, 93, 341-357.
4. F. Masamichi, S. Yoshiharu and O. Tetsuo, *Nature*, 1981, 293, 206-208.
5. K. Tomoji and S. Tadayoshi, *Nature*, 1980, 286, 474-476.
6. X. Fu, J. Long, X. Wang, D. Y. C. Leung, Z. Ding, L. Wu, Z. Zhang, Z. Li and X. Fu, *International Journal of Hydrogen Energy*, 2008, 33, 6484-6491.
7. C. Ampelli, R. Passalacqua, C. Genovese, S. Perathoner, G. Centi, T. Montini, V. Gombac, J. J. Delgado Jaen and P. Fornasiero, *RSC Advances*, 2013, 3, 21776-21788.
8. K. Shimura and H. Yoshida, *Energy & Environmental Science*, 2011, 4, 2467-2481.
9. X. Fu, X. Wang, D. Y. C. Leung, W. Xue, Z. Ding, H. Huang and X. Fu, *Catalysis Communications*, 2010, 12, 184-187.
10. M. R. St. John, A. J. Furgala and A. F. Sammells, *The Journal of Physical Chemistry*, 1983, 87, 801-805.
11. W. Y. Gan, D. Friedmann, R. Amal, S. Zhang, K. Chiang and H. Zhao, *Chemical Engineering Journal*, 2010, 158, 482-488.
12. A. Paracchino, V. Laporte, K. Sivula, M. Grätzel and E. Thimsen, *Nat Mater*, 2011, 10, 456-461.
13. Z. Zhang, R. Dua, L. Zhang, H. Zhu, H. Zhang and P. Wang, *ACS Nano*, 2013, 7, 1709-1717.
14. U. A. Joshi and P. A. Maggard, *The Journal of Physical Chemistry Letters*, 2012, 3, 1577-1581.
15. L. Zhang, J. Shi, M. Liu, D. Jing and L. Guo, *Chemical Communications*, 2014, 50, 192-194.
16. C. A. N. Fernando, L. A. A. D. Silva, R. M. Mehra and K. Takahashi, *Semiconductor Science and Technology*, 2001, 16, 433.
17. C. M. McShane, W. P. Siripala and K.-S. Choi, *The Journal of Physical Chemistry Letters*, 2010, 1, 2666-2670.
18. P. Adriana, L. Vincent, S. Kevin, G. Michael and T. Elijah, *Nature Materials*, 2011, 10, 456-461.
19. Q. Huang, F. Kang, H. Liu, Q. Li and X. Xiao, *Journal of Materials Chemistry A*, 2013, 1, 2418-2425.
20. B. Seger, T. Pedersen, A. B. Laursen, P. C. K. Vesborg, O. Hansen and I. Chorkendorff, *Journal of the American Chemical Society*, 2013, 135, 1057-1064.
21. D. Barreca, G. Carraro, E. Comini, A. Gasparotto, C. Maccato, C. Sada, G. Sberveglieri and E. Tondello, *The Journal of Physical Chemistry C*, 2011, 115, 10510-10517.
22. A. Heller and B. Feldman, *Accounts of Chemical Research*, 2010, 43, 963-973.
23. A. Devadoss, P. Sudhagar, S. Das, S. Y. Lee, C. Terashima, K. Nakata, A. Fujishima, W. Choi, Y. S. Kang and U. Paik, *ACS Applied Materials & Interfaces*, 2014, 6, 4864-4871.
24. M. Veerapandian, H. Y. Kim, Y.-T. Seo, K.-N. Lee, K. Yun and M.-H. Lee, *Materials Research Bulletin*, 2014, 49, 593-600.
25. L. Han, L. Bai, C. Zhu, Y. Wang and S. Dong, *Chemical Communications*, 2012, 48, 6103-6105.
26. R. M. Navarro, M. C. Sanchez-Sanchez, M. C. Alvarez-Galvan, F. d. Valle and J. L. G. Fierro, *Energy & Environmental Science*, 2009, 2, 35-54.
27. P. Poizot, C.-J. Hung, M. P. Nikiforov, E. W. Bohannan and J. A. Switzer, *Electrochemical and Solid-State Letters*, 2003, 6, C21-C25.
28. K. Khojier, H. Savaloni and Z. Sadeghi, *J Theor Appl Phys*, 2014, 8, 1-8.
29. J. H. Pan, Z. Lei, W. I. Lee, Z. Xiong, Q. Wang and X. S. Zhao, *Catalysis Science & Technology*, 2012, 2, 147-155.
30. Z. Luo, H. Jiang, D. Li, L. Hu, W. Geng, P. Wei and P. Ouyang, *RSC Advances*, 2014, 4, 17797-17804.
31. X. Y. Fan, Z. G. Wu, P. X. Yan, B. S. Geng, H. J. Li, C. Li and P. J. Zhang, *Materials Letters*, 2008, 62, 1805-1808.
32. J. P. Espinós, J. Morales, A. Barranco, A. Caballero, J. P. Holgado and A. R. González-Elipe, *The Journal of Physical Chemistry B*, 2002, 106, 6921-6929.
33. Q. Yu, X. Ma, Z. Lan, M. Wang and C. Yu, *The Journal of Physical Chemistry C*, 2009, 113, 6969-6975.
34. D. Tahir and S. Tougaard, *Journal of Physics: Condensed Matter*, 2012, 24, 175002.
35. K. Rajeshwar, N. R. de Tacconi, G. Ghadimkhani, W. Chanmanee and C. Janáky, *ChemPhysChem*, 2013, 14, 2251-2259.

36. M.-F. Wang, Q.-A. Huang, X.-Z. Li and Y. Wei, *Analytical Methods*, 2012, 4, 3174-3179.
37. Y. Wei, L. Ke, J. Kong, H. Liu, Z. Jiao, X. Lu, H. Du and X. W. Sun, *Nanotechnology*, 2012, 23, 235401.
38. X. Lu, S. Xie, H. Yang, Y. Tong and H. Ji, *Chemical Society Reviews*, 2014, DOI: 10.1039/c3cs60392j.
39. D. V. Esposito, R. V. Forest, Y. Chang, N. Gaillard, B. E. McCandless, S. Hou, K. H. Lee, R. W. Birkmire and J. G. Chen, *Energy & Environmental Science*, 2012, 5, 9091-9099.
40. G. Wang, Y. Ling, X. Lu, T. Zhai, F. Qian, Y. Tong and Y. Li, *Nanoscale*, 2013, 5, 4129-4133.
41. S. Xie, T. Zhai, W. Li, M. Yu, C. Liang, J. Gan, X. Lu and Y. Tong, *Green Chemistry*, 2013, 15, 2434-2440.